COBEM 2023 27TH INTERNATIONAL CONGRESS OF MECHANICAL ENGENEERING

ABCM Brazilian Society of Mechanical Sciences and Engineering
27th ABCM International Congress of Mechanical Engineering
December 04-08, 2023, Florianópolis-SC, Brazil

COB-2023-0726

ANALYSIS OF SEMI-ELLIPTICAL CRACK GROWTH IN PRESSURE VESSELS

Hallan Moura Ladeira
Carla Tatiana Mota Anflor

Group of Experimental and Computational Mechanics - GMEC, University of Brasilia
Emails:hallanmouraladeira@gmail.com; anflor@unb.br

Abstract. *The corrected text is: The present study investigates the stress in an ASTM 516 GR 70 steel pressure vessel and its relationship with the occurrence of semi-elliptical cracks near regions where the maximum principal stress acts with greater intensity. To illustrate this relationship, a case study using a reduced model of the pressure vessel is presented, focusing on the behavior of the semi-elliptical crack in the presence of discontinuities. The results demonstrate that the insertion of semi-elliptical crack close to the discontinuities can significantly modify the mode of crack propagation in those regions.*

Keywords: *fracture mechanics, pressure vessel, crack growth, stress concentration, computational modeling.*

1 INTRODUCTION

Mechanical failures initiated by cracks are technically irreversible phenomena that can have serious consequences on structural components. These cracks can arise due to several factors, including imperfections in the manufacturing process, voids in the casting, temporary manifestations, and geometric characteristics that lead to stress concentrators at specific points on the component (RAUL GASPARI SANTOS; EMERSON DOS REIS; RENATO CHAVES SOUZA, 2016). The presence of cracks in structures can lead to financial losses and catastrophic accidents, putting both individuals and processes at risk. In this sense, understanding the behavior of cracks is crucial in the context of fracture mechanics. Cracks can be categorized into three opening modes: Mode I involves separating the crack faces, Mode II involves sliding the crack faces, and Mode III involves shearing. Most crack-related engineering problems are focused on Mode I fractures, where crack growth occurs when the stress intensity factor (SIF) exceeds the fracture toughness of the material (KIc) under monotonic loading conditions (FUCHS; STEPHENS; SAUNDERS, 1981). Importantly, cracks originate at the atomic level and become detectable when they reach a minimum length of 1mm. Singularities in mechanical components, such as holes, are common stress concentration factors that can promote crack nucleation. Therefore, proper drilling techniques, ensuring size, shape and absence of burrs, are necessary to avoid localized failures close to the contact regions of the hole (ZHAO; JIANG, 2008).

In materials subjected to long-term maintenance and structural stress design, damage accumulates over time until it triggers the failure phenomenon. Even under low stresses, this gradual accumulation of damage can lead to degradation of the material, ultimately reducing its acceptable design levels (REIFSNIDER *et al.*, 2009). To prevent accidents and ensure the safety of people and processes, it is essential to carry out studies focused on the detection and monitoring of damage to structures. This includes implementing repairs that improve manufacturing processes, material selection, load types, and usage environments. Additionally, regular inspections and failure analysis of equipment and structures are critical to maintaining safety.

In (BURDEKIN, 1982) four vessel failures due to fracture reveals the presence of multiple factors involved in such occurrences. Material properties, heat treatment, manufacturing methods, and non-destructive testing are key factors that require strict quality control. By giving full attention to these aspects and the overall basic design, fracture mechanics emerges as an important tool to help determine material requirements, manufacturing standards, and assess the overall probability of failure.

A fracture study in a Pressure Vessel (RPV) reactor was conducted using finite element analysis in (ZHENG et al., 2023). The results obtained by the authors revealed that, as the depth/thickness ratio of the crack increases and the ratio of the crack aspect to (w/c) decreases, there is an overall increase in the level of crack restriction. For most cracks with a/t = 0.25-0.8 and a/c = 0.2-2, the restriction level exceeds that of the standard plane strain specimen. This finding suggests the possibility of non-conservative fracture evaluations. In addition, the results highlight the significant influence of the crack aspect ratio on the distribution of restriction parameters and fracture onset positions along the crack fronts.

Fracture mechanics provides an important tool for assessing material requirements, manufacturing standards, and the overall likelihood of failure in structural components. It allows a rational index for the approach of complex and uncertain problems, aiding decision-making processes (KANTO *et al.,* 2010). Recent activities of the Japanese research group Probabilistic Fracture Mechanics (PFM) have made significant contributions to the field over the past two decades. Their research efforts, which began with surveys of the literature, have yielded fruitful results and several original MAP programs. These activities have extended the application of PFM to various components and problems in nuclear power plants, including economic basis analyses. This demonstrates the potential of PFM as a valuable tool for optimizing decision-making processes in complex scenarios.

The Japanese PFM research group has also conducted several round-robin analysis programs, with the aim of enhancing knowledge and experience of PFM techniques among its members. These efforts fostered collaboration and knowledge sharing within the group, and in 2008 the initiative was extended to international research groups in Korea and Taiwan. Ongoing research and collaboration activities reflect the group's commitment to advancing PFM and its practical applications.

In the context of pressure vessels, the presence of holes can significantly affect the stress distribution and increase susceptibility to crack initiation, leading to component failure. Therefore, this study aims to validate a geometric model used in previous research (SILVA, 2015) by performing numerical analyses using the Finite Element Method (FEM). Specifically, the equivalent von Mises stress will be compared between the original and reduced models of an ASTM 516 GR 70 steel pressure vessel. Boundary conditions will also be studied to optimize computational efficiency and evaluate crack behavior.

By conducting this research, we aim to contribute to the advancement of knowledge of fracture mechanics and provide valuable information to optimize the processes of design and evaluation of the integrity of pressure vessels. The results will not only increase our understanding of stress fields in pressure vessels with the presence of boreholes, but also allow for better risk assessment and mitigation strategies to ensure the safety and reliability of such critical components.

The present research is carried out with the objective of assisting in the resolution of linear elastic fracture mechanics problems in pressure vessels. The objective is to analyze the influence of boreholes and monitor the growth and opening behavior of semi-elliptical cracks near this region in order to take measures to reduce the risk of catastrophes.

2 MATERIALS AND METHODS

2.1 Model Validation

In this study, the model previously studied by (SILVA, 2015) was considered as a benchmark. The objective in this section is to analyze the stress field in a horizontal pressure vessel in ASTM 516 GR 70 steel, following the ASME and NR-13 standards. This study validated the model by numerical analysis using the Finite Element Method (FEM), based on the geometric references and material properties of the pressure vessel.

2.1.1 Mechanical properties and geometric model

The chemical composition of ASTM A516 Grade 70 steel and the characteristics of the pressure vessels are presented in Table 1 and Table 2, respectively.

Table1. Composition table for ASTM A516 Grade 70 steel.

	C (%)	Mn (%)	P (%)	S (%)	Si (%)
ASTM A516	0.27	0.85 – 1.20	0.035	0.035	0.15 – 0.40

Table 2. The characteristics of the pressure vessel.

Description	Dimensions
Inner diameter of the vessel	3400 mm
Vase Length	9200 mm
End Plugs	According to ASME 2:1 Ellipsoidal
Design Pressure	10 MPa
Tolerance for Corrosion Thickness	6 mm

Additional pressure vessel components/accessories are introduced in Table 2, while Figure 1 shows a schematic representation of the component assembly.

Table 3. Pressure vessel fittings.

Components	Diameter (mm)	Thickness (mm)
ASME Ellipsoidal 2:1 Head	3400	160
Side	3400	160
Main Entrance	660.40	38.10
Visiting Room	609.60	38.10
Low Output	304.80	20.637
High Output	304.80	20.637
Drain Well	760	38.10
Reinforcement Area	81280mm²	25.40

Note: (*) This measurement is given in square millimeters (mm²) and represents the sum of the radius of 161 mm, the radius of the orifice, and the thickness of the neck wall.

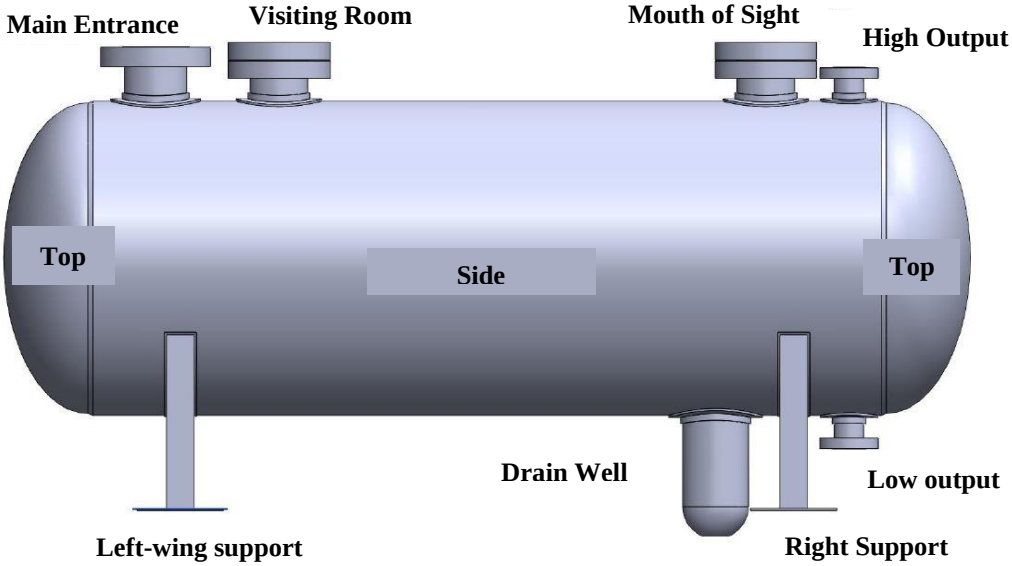

Figure 1. Schematic view of pressure vessel assembly.

3 Numerical results

3.1 Mesh Convergence Study

In the present study, the element quality technique was adopted to verify the metric of the tetrahedral mesh of the pressure vessel, which is calculated as the ratio between the largest dimension (longest edge) and the smallest dimension (shortest edge) of the element. According to the ratio mesh metric, the closer the value is to 1, the better the mesh quality, as shown in Figure Figure 2

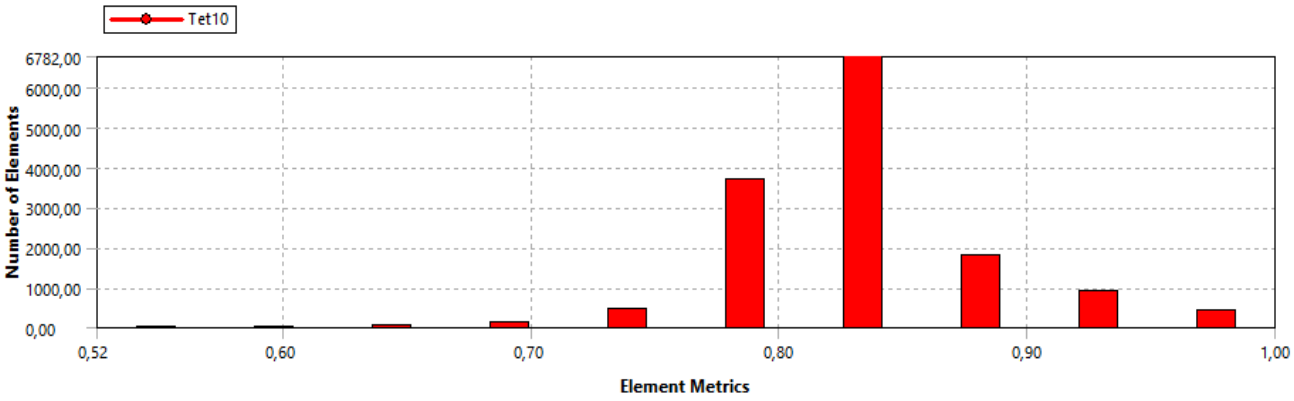

Figure 2. Mesh metric.

The equation employed to calculate the mesh metric according to the element quality are introduced in equation 1. The constants for the mesh quality used in equation 1 are available in Table 4.

$$Quality = C\left[\frac{VOLUME}{\sqrt{(\sum[\![(Edge\ length)^2)]\!]^3}}\right] \quad \textbf{(1)}$$

Table 4. Constants for Mesh Quality Determination

Elements	Values of C
Triangle	6.92820323
Square	4.0
Tetrahedral	124.70765802
Hexagon	41.56921938
Wedge	62.35382905
Pyramid	96

The metric mesh study was performed for the pressure vessel, using quadratic analysis with three degrees of freedom per node. The objective was to ensure the accuracy of the stress distribution information for the number of elements in the mesh, evaluating the stability of the results of the Figure 3.

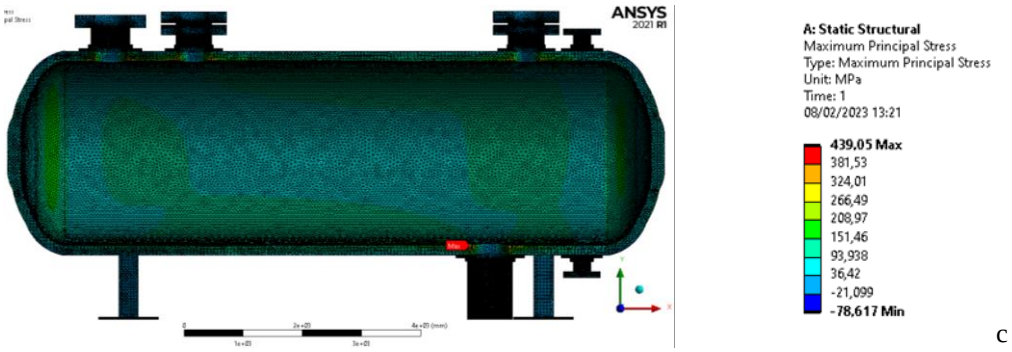

c

Figure 3. Vessel maximum principal stress field.

A comparative analysis (Figure 4) showed that the increase in the number of elements and knots did not significantly affect the equivalent von Mises stress. Based on these results, the mesh with element sizes ranging from 5 to 60mm was chosen due to its lower computational cost and reliable results. This selection achieved a balance between the reliability of the results and the computational efficiency, contributing to the advancement of pressure vessel design.

The analyses showed that the elements that make up the mesh do not induce significant changes in the maximum variation of the stress field. Throughout the evolution of the study, among the mesh studies performed, the model with 3.770.800 elements and 5.516.900 nodes was selected. This choice was based on its lower computational cost and the absence of substantial deviations in stress analysis.

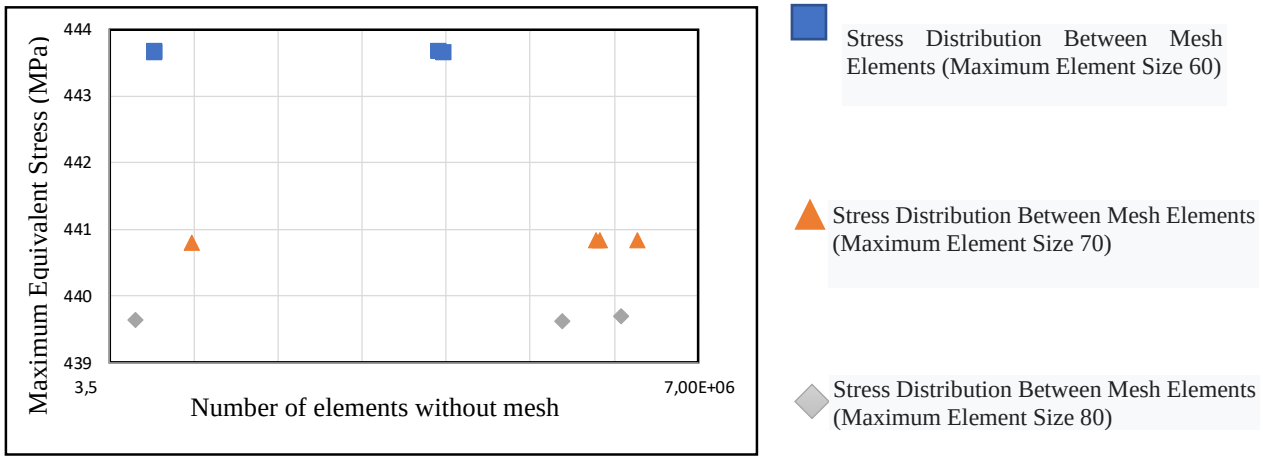

Figure 4. Tension equivalent to the number of elements in the mesh.

Figure 5 shows the region where the maximum principal stress occurs within the pressure vessel, and those close to the Drain Well are more susceptible to the appearance of cracks.

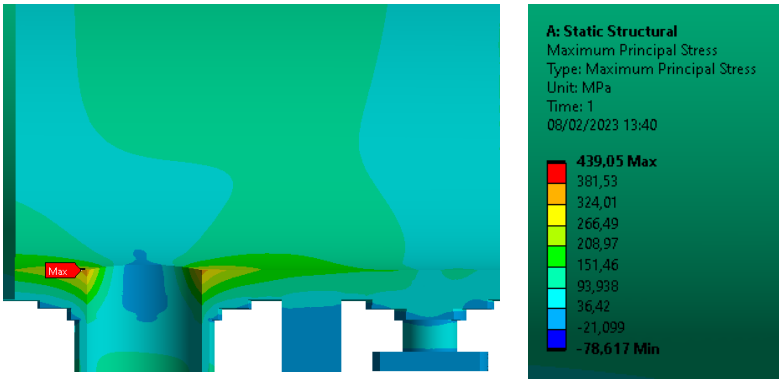

Figure 5. Maximum principal stress at the Drain Well region.

3.2 Comparison between the benchmark and the current model.

The design model studied followed the parameters, references, and physical conditions studied by (SILVA, 2015). Replicating the author's work, a numerical study was carried out to obtain the stress results of the studied model. The objective was to validate the results in order to continue the work. The material for the pressure vessels was ASTM 516 Gr 70 steel, and the physical properties can be found in Table5.

Table5. Physical properties of the material.

Ultimate Stress	620MPa
Yield Stress	260MPa
Allowable Stress	138MPa
Poisson ratio	0.3
Fracture toughness	37.6MPa√mm

3.3 The Boundary Conditions.

The boundary conditions for the pressure vessel supports and accessories can be seen in Table 6.

Table 6. Boundary Conditions.

Boundary Conditions	
Conditions	Restrictions.
Left vessel support	Fixed
Vessel Right Support	Offset in X direction
Main Entrance	Offset in X and Z directions
Taken	Offset in X and Z directions
Ship's Inner Surface	Pressure
Fundamental Strength	Gravity in the Y direction

3.4 Stress Field Analysis

The comparison between (SILVA, 2015) and the present model allowed the validation of the stress field, showing a variation of approximately 10.49% between the stresses of both pressure vessels according to equation 2 and equation 3, see Table 7Table7. The degree of confidence in the results obtained in this study is approximately 90%. The stress field for both models can be seen in Figure 6, while Figure 7 introduces the isolines for the maximum principal stress at the Drain Well region.

$$Variation = 443.64\ MPa - 397.07\ MPa = 46.56\ MPa \quad \textbf{(2)}$$

$$relative\ difference\ = 100 - \left(\frac{397{,}07\ MPa}{443{,}63\ MPa} * 100\right) \approx 10.49\% \quad \textbf{(3)}$$

Table7. Comparison of the von Mises stress for both models

Maximum Equivalent Stress [MPa]			
Silva (2015) ·	Current work	Variation [MPa]	Relative difference [%]
397.07	443.63	46.56	10.49

The study conducted by (SILVA, 2015) evaluated the distribution of the Von Mises stress field within the examined pressure vessel. The purpose of this current research was to achieve acceptable results for the continuation of the study, thereby obtaining approximate stress distribution values and validating the model previously examined by Silva. This validation brings confidence to the present study, ensuring the credibility of the undertaken analyses.

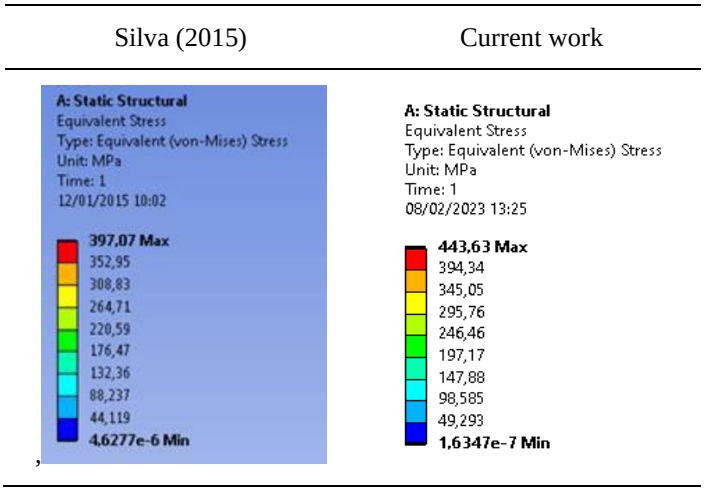

Figure 6. Comparison of the von Mises stress for both cases.

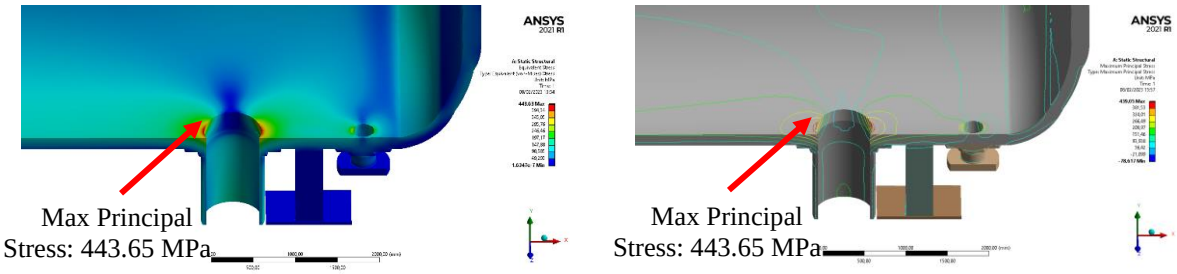

Figure 7. Maximum principal stress.

3.5 The Boundary Conditions.

The original pressure vessel model was reduced to a curved plate to minimize computational efforts, adopting fixed support boundary conditions. The path command, available in ANSYS, was used to track the stress values in the region where the line was positioned. The track line was employed for the reduced and the complete model.

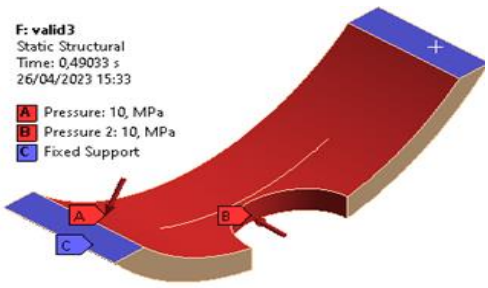

Fixed Support

Figure 8. The boundary conditions.

3.6 Linear Elastic Fracture Mechanics applied to the vessel

The pressure vessel is subject to loads in all directions, the inner fibers are kept under compression, while the outer fibers are subjected to tension. In this sense, there is a greater probability of cracks occurring in the external region in relation to the internal region of the vessel Figure 9.

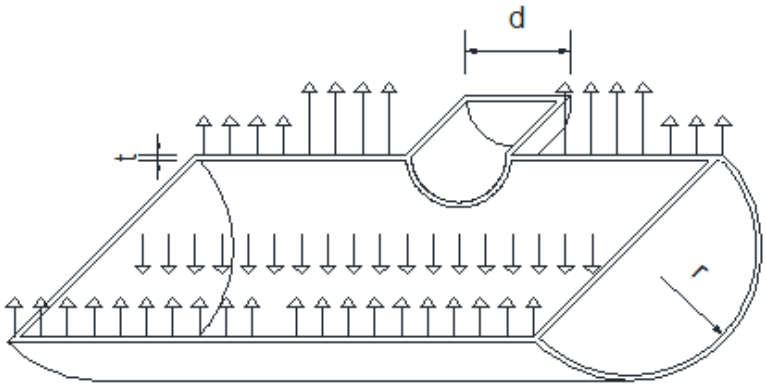

Figure 9. Pressure vessel loads.

Stress concentration factors significantly increase the likelihood of cracks occurring in their vicinity. Therefore, in order to investigate this phenomenon, attention was focused on the growth of the crack in the traction region of the pressure vessel, specifically near the borehole. In this region, the crack behavior can be observed in three different opening modes (mixed mode), since the vessel walls are subjected to stresses in all directions. The crack initially develops in mode one of opening and then evolves to modes two and three, resulting in a loss of section that weakens the vessel wall structure.

Figure 10 illustrates the semi-elliptical crack growth pattern in a pressure vessel near the stress concentration region. This area is prone to higher levels of stress, leading to crack initiation and propagation. A crack tends to propagate in a specific direction, following the path of least resistance in the material. This crack growth pattern is of particular interest in understanding the structural integrity and rupture mechanisms of pressure vessels. Figure 12 to Figure 14 provide a comparison of SIFs (K_1, K_2, and K_3) for scenario a) where the crack initiates at 0.77941 mm and reaches its maximum size in scenario b) at length of 27.466 mm.

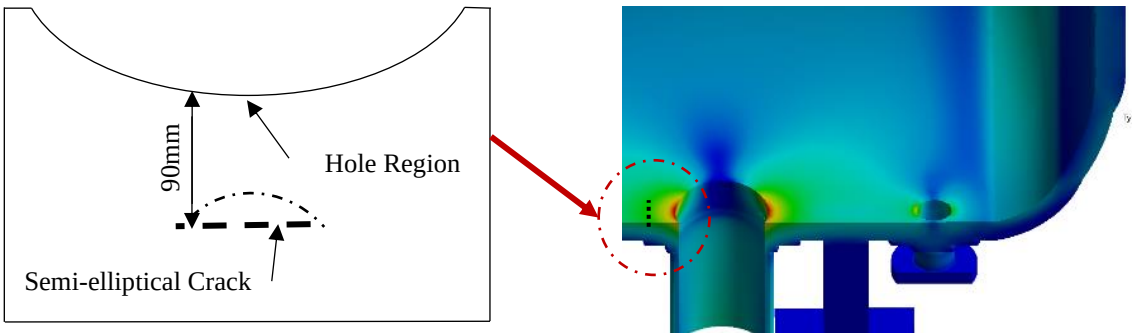

Initial crack length = 0.77941mm
Final crack length = 27.466mm

Figure 10. Initial position of the crack.

Figure 11 introduces the crack growth for each iterative process (steps *vs* crack length). In this work, for effect of study the crack growth was allowed to reach a maximum length around of 27mm. In Figure 12, the evolution of K_1 is depicted as the crack grows from its initial size (Figure 12a) to its final size (Figure 12b). It's important to highlight that at initial length of the crack (Figure 12a) the mode K_1 presents the both Plane Stress and Plane Strain State. At Figure 12b, the SIF graph presents a different behavior when compared to the Figure 12a, because the remaining modes K_2 and K_3 are taking effect over the crack propagation.

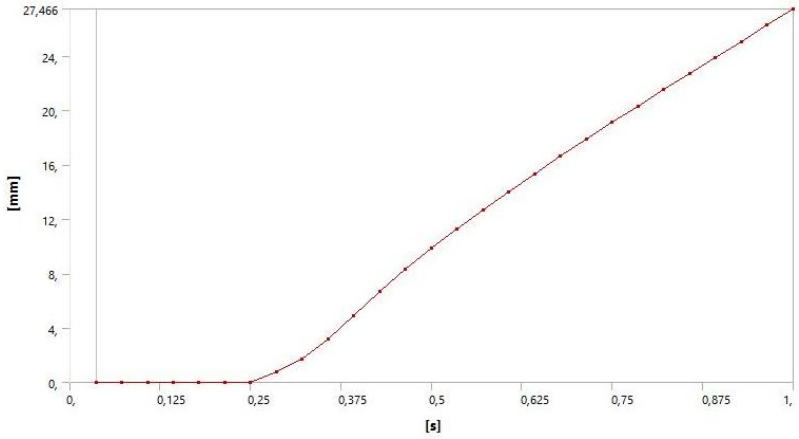

Figure 11.Graph Crack Growth.

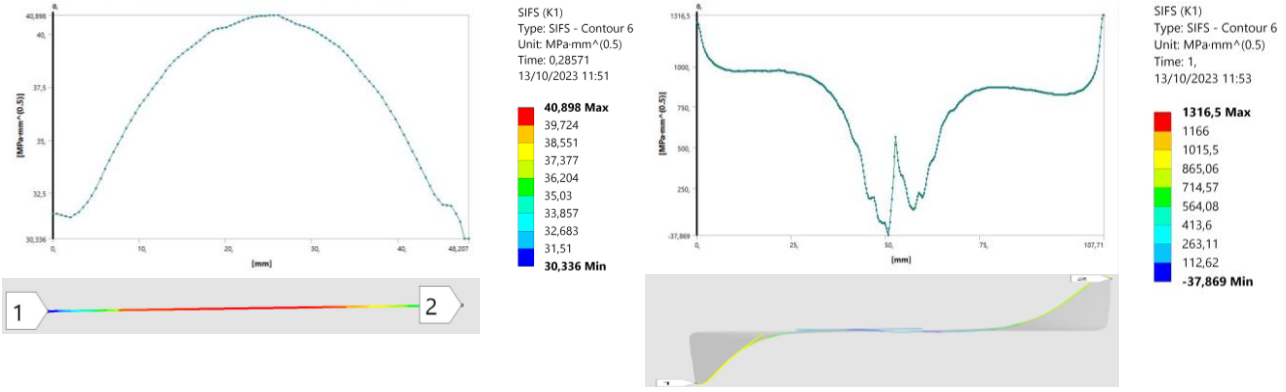

a) Initial Crack length 0.77941mm b) Final Crack length 27.466mm

Figure 12. Evolution Crack Growth of K_1.

In Figure 13, one can appreciate the mode K_2 behavior introduced for the initial and the final length of the crack. At the initial crack length (Figure 13a) the influence of mode K_2 is almost negligeable (3.3076 MPamm^0.5), evolving to 58.107 MPamm^0,5 at the final length of 27.466mm. Analyzing Figure 13a and 13b it's possible to observe the increase of the slipping effect due to the increase of the semi-elliptical crack length (from 48.207mm to 107.71mm).

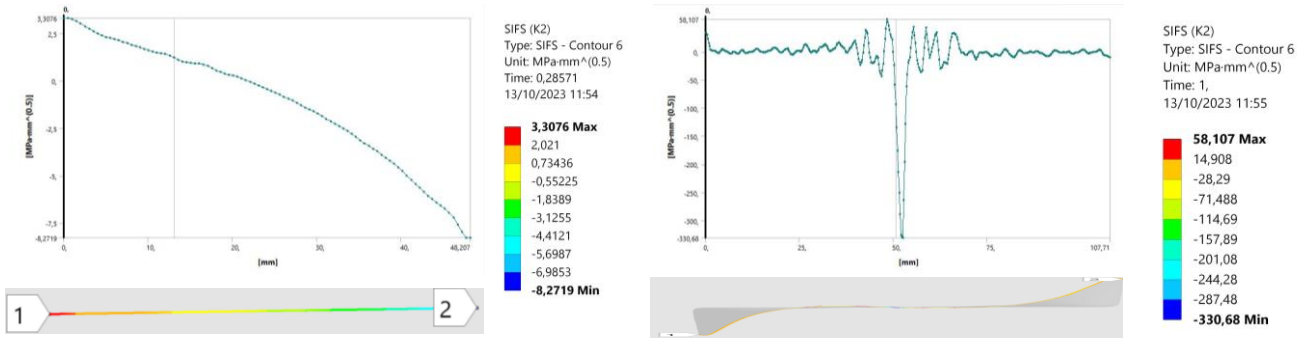

a) Initial Crack length 0,77941mm b) Final Crack length 27,466mm

Figure 13. Evolution Crack Growth of K_2.

Figure 14 shows graphs for mode K_3, providing a measure of shear effect at the crack tip. As mentioned in the K_2 mode (Figure 13), the mode K_3 also take a significant effect as the crack increase and the shear effect is responsible for the change of the crack shape (ranging from 14.54MPamm^0.5 to 459.43 MPamm^0.5).

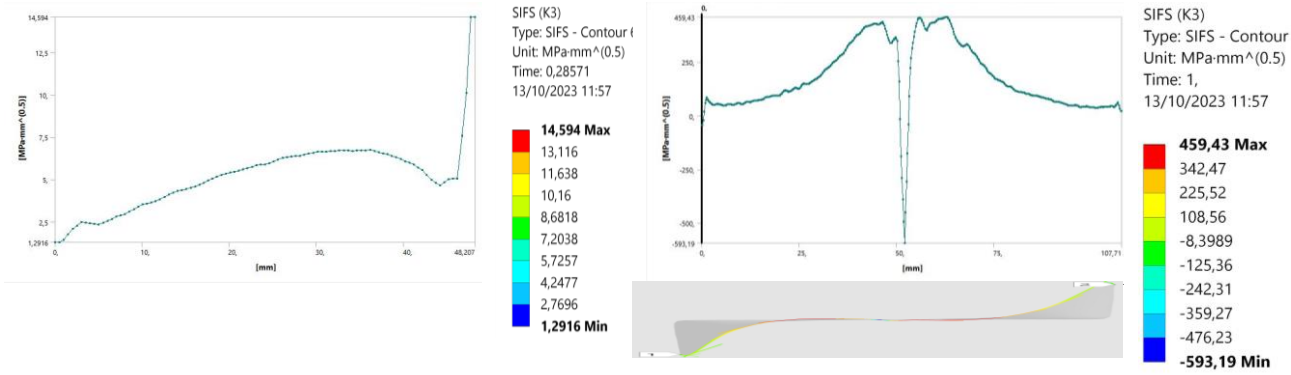

a) Initial Crack length 0.77941mm b) Final Crack length 27.466mm

Figure 14. Evolution Crack Growth of K_3.

4 CONCLUSION

This study highlights that semi-elliptical crack close to the stress concentration have a greater tendency to propagate changing from opening mode I to mixed mode. The process of crack growth resulted in a reduction in the cross-sectional area of the vessel walls, which can lead to catastrophic consequences due to the loss of strength of the material. It is important to note that although thick walls can withstand internal pressure in the pressure vessel, the crack does not pass through, but grows along the contour of the vessel, reducing the cross-sectional area of the material. This can significantly decrease the load-bearing capacity of the part, increasing the risk of catastrophic failures. In addition, this type of analysis can provide information for the application of the Leak-Before-Break theory by defining the width of the pressure vessel appropriately. Therefore, it is essential to adopt preventive measures, such as conducting regular inspections, identifying and monitoring cracks early, and using resilient materials and design techniques that minimize stress concentration. These measures aim to ensure the structural integrity of the pressure vessel, prevent serious accidents, and preserve the safety of the industrial systems in which they are employed. Finally, further investigations will be carried out to address the current vessel problem, taking into account crack growth due to fatigue caused by alternating stress.

5 ACKNOWLEDGEMENTS

The first author would also like to thank the support received from the Coordination for the Improvement of Higher Education Personnel (CAPES) and the Research Support Foundation of the Federal District (FAP-DF) for their contribution to the work. The second author expresses her gratitude to the National Council for Scientific and Technological Development (CNPq) for granting the scholarship with reference number 314602/2021-6.

6 REFERENCES

BURDEKIN, F. M.; The role of fracture mechanics in the safety analysis of pressure vessels. *International Journal of Mechanical Sciences*, v. 24, n. 4, p. 197–208, 1982.

OLIVEIRA, A. O.; OLIVEIRA, R. I.; SAUNDERS, H. *Fatigue of Metals in Engineering (1980)*. [S.l: s.n.], 1981. v. 103.

KANTO, Y. *et al.* Recent Japanese research activities on probabilistic fracture mechanics for pressure vessels and nuclear power plant pipelines. *International Journal of Pressure Vessels and Pipes*, v. 87, n. 1, p. 11–16, 2010. Available at: <http://dx.doi.org/10.1016/j.ijpvp.2009.11.010>.

RAUL GASPARI SANTOS; EMERSON DOS REIS; RENATO CHAVES SOUZA. Techniques for identification of the initial stage and/or follow-up of cracks caused by mechanical fatigue. *Proceedings of the IX National Congress of Mechanical Engineering*, n. March 2018, 2016.

REIFSNIDER, K. L. *et al.* Alterations of the material state as a basis for prognosis in aeronautical structures. *Aeronautical Journal*, v. 113, n. 1150, p. 789–798, 2009.

SILVA, Adson Beserra Da. Pressure vessel design according to ASME standard and finite element method analysis. p. 141, 2015.

ZHAO, Tianwen; JIANG, Yanyao. Aluminum alloy 7075-T651 fatigue. *International Journal of Fatigue*, v. 30, n. 5, p. 834–849, 2008.

ZHENG, Y. *et al.* Characterization of constraints and fracture initiation analysis for semi-elliptic surface cracks in a reactor pressure vessel. *International Journal of Pressure Vessels and Pipes*, Vol. 202, No. November 2022, 2023.